

A Polymer Cable Creep Modeling for a Cable-Driven Parallel Robot in a Heavy Payload Application

Jinlong Piao^{1,2}, XueJun Jin^{1,2}, Eunpyo Choi^{1,2}, Jong-Oh Park^{1,2}(✉),
Chang-Sei Kim^{1,2}, and Jinwoo Jung²(✉)

¹ School of Mechanical Engineering,
Chonnam National University, Gwangju, South Korea
piaojinlong622@163.com, harkjoon27@gmail.com,
eunpyochoi@chonnam.ac.kr, {jop, ckim}@jnu.ac.kr

² Medical Microrobot Center, Robot Research Initiative,
Chonnam National University, Gwangju, South Korea
{eunpyochoi, jwjung}@chonnam.ac.kr

Abstract. A polymer cable driven parallel robot can be an effective system in many fields due to its fast dynamics, high payload capability and large workspace. However, creep behavior of polymer cables may yield a posture control problem, especially in high payload pick and place application. The aim of this paper is to predict creep behavior of polymer cables by using different mathematical models for loading and unloading motion. In this paper, we propose a five-element model of the polymer cable that is made with series combination of a linear spring and two Voigt models, to portray experimental creep in simulation. Ultimately, the cable creep can be represented by payloads and cable length estimated according to the changes of actual payloads and cable lengths in static condition.

Keywords: Cable suspended parallel robot · Polymer cable · Creep · Parameter identification

1 Introduction

A cable-driven parallel robot (CDPR) is a parallel robot whose end-effector is controlled by winding and unwinding flexible cables. Unlike a robotic system with rigid body links, the use of flexible light cable or rope as actuator can significantly reduce actuator weight, thus CDPR has the advantages in the application of heavy materials handling and larger workspace with low cost [1–4]. Although the CDPR as a modified version of robotic cranes has a potential of effective applications, viscoelastic property of cable yields accuracy problems while position or tracking control.

The cable modeling has been motivated by several researchers to develop cable models to overcome issues in using the flexible cable as an actuator of robotic system. Kraus et al. use a computationally efficient and real-time applicable model to identify payload, estimate the end-effector position and compensate position error. Their stiffness model can reduce position errors caused by cable elasticity [5]. Also hysteresis

behavior of cable driven system has been studied by Miermeister et al. who developed an improved cable model including the hysteresis effect during cable force computation. In order to avoid a complex distributed parameter model, they used a black box model to represent the cable [6]. M. Miyasaka et al. developed the hysteresis model for longitudinally loaded cables based on the Bouc-Wen hysteresis model. Also, the model is capable of emulating thin *and thick stainless* steels used for the RAVEN II system and its parameters were optimized using the genetic algorithm [7]. In addition, the elasticity and uncertainties of a CDPR can be neutralized by robust control. M.H. Korayem compensated the flexibility and uncertainties of cable suspended robot using sliding mode control [8]. Those approaches has improved tracking performance of CDPR obviously. However, there is considerable cable creeping behavior in specific applications, such as high precision part assembly and high payload pick and place application. Thus, using a creep model can improve performance of CDPR. In this paper, we propose a five-element model to properly describe significant experimental creep.

This paper is organized as follow. First, the development of a high payload cable robot is briefly described. Second, a five-element model is introduced for describing experimental creep. Third, experimental results for showing creep behavior are discussed for building a creep model. Fourth, via surface fitting process, the parameters estimation results for the suggested model based on the experimental data by different payloads and cable lengths will be shown. Finally, conclusion and future work will be discussed.

2 CNU Cable Robot System and Creep Experiments

2.1 CNU Cable Robot System

The high payload CDPR, shown in Fig. 1, is developed for the purpose of heavy part assembly and pick and place application. The size of base frame is $4\text{ m} \times 4\text{ m} \times 4\text{ m}$ and eight pulleys are fixed near the corners of top frame. Configurations of cable connection were designed for a wider workspace [9]. Maximum payload that the robot can manipulate is 65 kg and the goal of this robot is to have capability of handling more than 200 kg.

As a light flexible actuator of the high payload cable robot system, polyethylene Dyneema[®] cable, LIROS D-Pro 01505-0600, are used. The weight of cable is 1 kg/100 m with a diameter of 6 mm. Polyethylene cable has an advantage of light-weight compared to steel cable in industrial application. However, it may cause a concern of viscoelastic behavior such as creep in loading and unloading motion.

2.2 Cable Creep Experiment

When a polymer cable is subjected to load and unload a heavy object, it exhibits time dependent elongation characteristic called creep behavior. There are several factors influencing creep behavior of a polymer cable, such as type of material property, weight of load, length of cable and temperature. Although temperature is one of the important factors that can accelerate cable creep behavior, we only consider the load

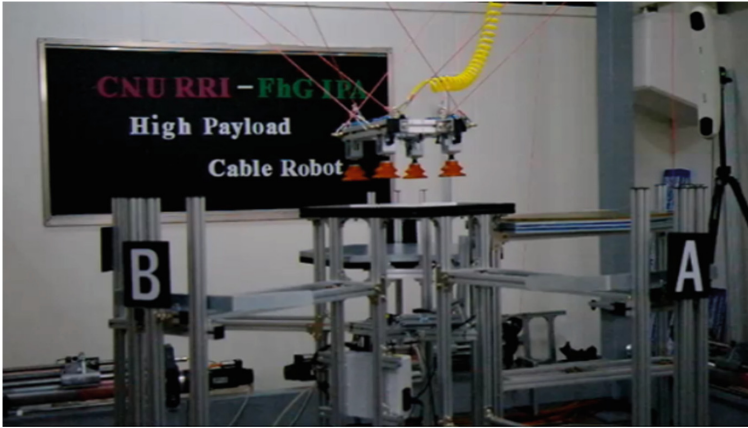


Fig. 1. High payload CDPR

weight and cable length in our experiment by assuming that our system is operated in a room temperature. In order to measure cable creep behavior in experiments, creep tests for the actual CDPR cable are conducted. There are various kinds of creep testing equipment that are most commonly used in experiments to create a creep curve [10]. However, it is difficult to realize different loading and unloading behavior happened while heavy load handling for the actual cable driven robot system. Tensile testing machine can express strain-stress curve of materials [11], but it is also not easy to test long length of cables due to the hardware limitations. Then, we used actual winch-cable-pulley system and a crane for loading and unloading weight blocks to measure cable creeping behavior because it can handle high weight and long cable lengths.

The experimental setup for the creep test is shown in Fig. 2. We employed two different experiments for different loads and lengths shown in Figs. 2 and 3 respectively. For a fixed cable length, different payloads are applied one by one and repeated for other length cable with the same payload conditions, and all the measurements are acquired simultaneously.

As shown in Fig. 2, the cable starts from the fixed winch and pass through the pulleys to the hook in the testing mass. For loading, the crane moves down and for unloading, the crane moves up to the initial position. The displacement sensor, an optical tracking system (OTS) from NDI with a root mean square (RMS) of 0.3 mm resolution is used and its sensor tool with four ball markers are fixed at the cable.

In Fig. 2, we have nine weight blocks and the total sum of loads can be more than 100 kg including middle bar. And shown in Fig. 3, we have conducted cable length tests for three different cable lengths, 5.4 m, 7.4 m and 8.4 m, considering our current system configuration and operating ranges.

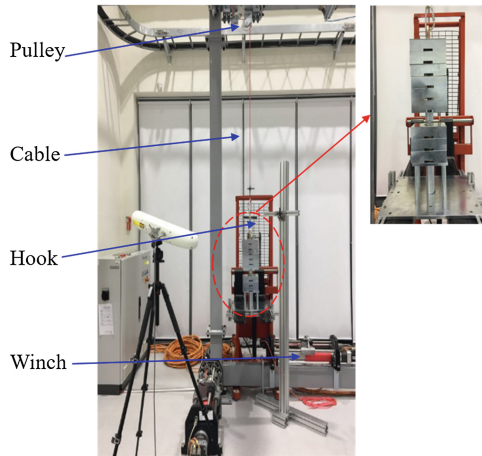


Fig. 2. Experimental setup with nine weight blocks

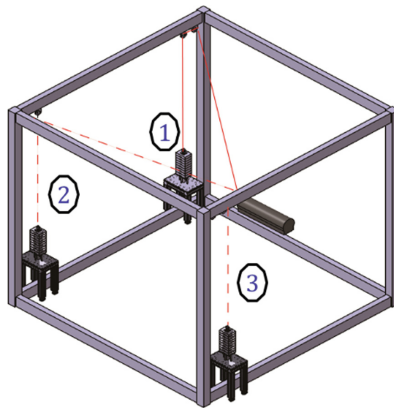


Fig. 3. Experimental setup with three different cable lengths

3 Creeping Modeling and Parameters Estimation

3.1 Cable Creep Modeling

A well-known very simple model that can describe creep behavior is a Voigt model. It consists of a Hookean spring and a Newtonian dashpot, but it does not fully explain complex experimental creep behavior in real system. In general, Burgers model can be used for describing complicated creep behavior [12]. This model is the serial combination of a Maxwell model and a Voigt model. However, by using Burgers model, it is also difficult to express long term creep behavior of polymer cable during unloading period.

In order to properly emulate long term creep behavior, we propose a five-element model based on Burgers model whose time-response can emulate three different time dependent behavior of a polymer cable. The model is the serial combination of a linear spring and two Voigt models, as shown in Fig. 4. According to the superposition principle the creep of cable is the sum of instantaneous elastic response, transient creep and long term creep [13]. Also, the creep behavior of loading and unloading can be different and therefore we use different model parameters indicated by subscripts Li and ULi. From loading $t = 0$ to unloading $t = t_r$, creeping behavior can be modeled as

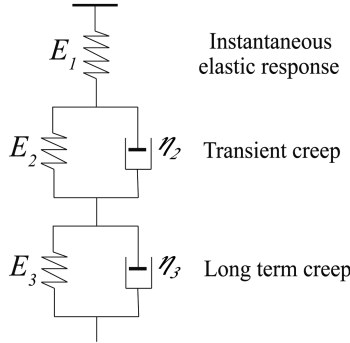


Fig. 4. A five-element model for cable creeping.

$$\varepsilon(t) = \frac{\sigma}{E_{L1}} + \frac{\sigma}{E_{L2}} \left(1 - e^{-\frac{E_{L2}t}{\eta_{L2}}}\right) + \frac{\sigma}{E_{L3}} \left(1 - e^{-\frac{E_{L3}t}{\eta_{L3}}}\right), \quad t = 0 \text{ to } t_r \quad (1)$$

where σ is the applied stress and ε is the strain of the cable. The model has five parameters in steady creep which are elastic modulus E_1 , E_2 , and E_3 for elastic property, transient creep, model and long-term creep effect, respectively and viscosity η_2 and η_3 for transient creep and long-term creep phenomena.

If the stress σ is removed when unloading the payload at $t = t_r$, $-\sigma$ can be added to (1). In the beginning of unloading, the negative stress applied to the cable increases up to $-\sigma_0$ until unloading completes ($t_r \leq t < t_2$) and remains as constant value $-\sigma_0$ ($t_2 \leq t$). Thus, strain recovery can be mathematically modeled as

$$\varepsilon(t) = \frac{\sigma_0}{E_{UL1}} + \frac{\sigma_0}{E_{UL2}} \left(1 - e^{-\frac{E_{UL2}t}{\eta_{UL2}}}\right) + \frac{\sigma_0}{E_{UL3}} \left(1 - e^{-\frac{E_{UL3}t}{\eta_{UL3}}}\right) + \left(\frac{\sigma}{E_{UL1}} + \frac{\sigma}{E_{UL2}} \left(1 - e^{-\frac{E_{UL2}(t-t_r)}{\eta_{UL2}}}\right) + \frac{\sigma}{E_{UL3}} \left(1 - e^{-\frac{E_{UL3}(t-t_r)}{\eta_{UL3}}}\right) \right), \quad t = t_r \text{ to } t_2, \quad \sigma = 0 \text{ to } -\sigma_0 \quad (2)$$

$$\varepsilon(t) = \frac{\sigma_0}{E_{UL2}} \left(e^{\frac{E_{UL2}t_r}{\eta_{UL2}}} - 1\right) e^{-\frac{E_{UL2}t}{\eta_{UL2}}} + \frac{\sigma_0}{E_{UL3}} \left(e^{\frac{E_{UL3}t_r}{\eta_{UL3}}} - 1\right) e^{-\frac{E_{UL3}t}{\eta_{UL3}}}, \quad t = t_2 \text{ to ending time} \quad (3)$$

3.2 Individual Model Parameters Estimation: Polynomial Fitting

Figures 5 and 6 show the experimental creep responses and the predictions of the five element model under a series of payloads and cable lengths, respectively. Experimental results show that creep behavior becomes more obvious with higher payload and longer cable length. Experiments also show that the creep behavior of loading and unloading is different. The creep behavior of unloading period is more obvious than that of loading period. In order to portray experimental creep, the five element model is used and the parameters of creep model are estimated by minimizing root mean square error (RMSE) between experimental data and model's output via brutal model parameter searching. Estimated parameters show that five parameters are changing in terms of different payloads and different cable lengths. Also, parameters are different with loading and unloading periods. In order to minimize the complexity of the model, we fixed less changed parameters when fitting experimental data and estimated the rest of parameters again as shown in Tables 1 and 2. Figures 5 and 6 show that the predictions of our model match with experiment data which the creeping behavior is different with different loads and cable lengths, also different when loading and unloading. These differences can be caused by nonlinear property of polymer cable. Also, loading weight has an influence on the cross sectional area of cable and changes the cable properties which can be illustrated using (4)

$$E = \frac{F/L_0}{A_0\Delta L} \quad (4)$$

where E is elastic modulus, F is the force exerted on the cable, A_0 is the actual cross-sectional area through which the force is applied, ΔL is the amount by which the length of the cable changes and L_0 is the original length of cable.

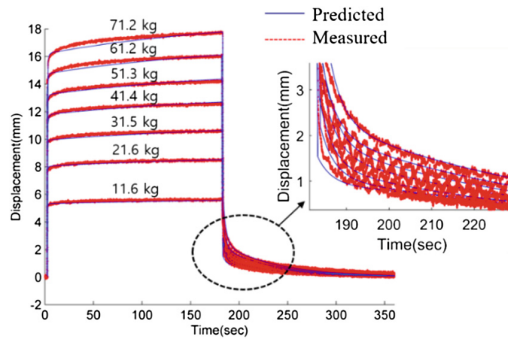


Fig. 5. Experimental creep responses and the predictions of the five element model under a series of payloads

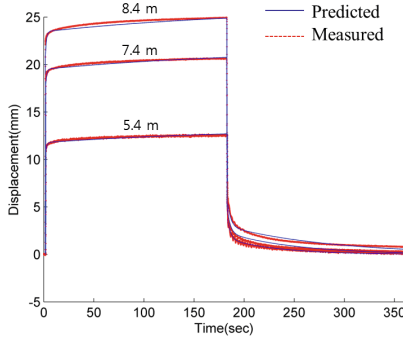


Fig. 6. Experimental creep responses and their predictions under a series of cable lengths

3.3 Dual Model Parameters Estimation: Surface Fitting

According to the experiments and estimated parameter, model parameters are influenced by loads and cable lengths. Thus, model parameters can be expressed as a function of mass (m) and cable length (l). Mass and length are utilized for the function instead of stress and strain because mass and cable length can be directly measured using force sensor and encoder equipped in our CDPR.

Table 1. Loading parameters

Parameters	Values	
Elastic modulus (N/m^2)	E_{L1}	$E_{L1}(m, l)$
	E_{L2}	9.5×10^9
	E_{L3}	5.0×10^{10}
Viscosity ($N \cdot s/m^2$)	η_{L2}	1.0×10^{10}
	η_{L3}	1.0×10^{13}

Table 2. Unloading parameters

Parameters	Values	
Elastic modulus (N/m^2)	E_{UL1}	$E_{UL1}(m, l)$
	E_{UL2}	$3.5 \times 10^{10} (N/m^2)$
	E_{UL3}	$E_{UL3}(m, l)$
Viscosity ($N \cdot s/m^2$)	η_{UL2}	$1.1 \times 10^{11} (N \cdot s/m^2)$
	η_{UL3}	$\eta_{UL3}(m, l)$

Table 1 and 2 show different parameters under loading and unloading respectively. The loading parameters E_{L2} , E_{L3} , η_{L2} , η_{L3} have constant values and E_{L1} is a function of mass (m) and cable length (l). The unloading parameter E_{UL2} , η_{UL2} are constant values and E_{UL1} , E_{UL3} , η_{UL3} are also a function of mass (m) and cable length (l).

Table 3. Polynomial model parameters

	E_{L1}	E_{UL1}	E_{UL3}	η_{UL3}
p_{00}	-5.036×10^{10}	-1.342×10^9	-8.301×10^{10}	2.803×10^{12}
p_{10}	3.07×10^9	5.933×10^8	-1.293×10^9	-1.993×10^{11}
p_{01}	1.81×10^{10}	2.052×10^9	2.799×10^{10}	-7.127×10^{11}
p_{20}	2.519×10^7	1.897×10^4	-9.385×10^6	2.543×10^9
p_{11}	-9.892×10^8	-1.438×10^8	8.516×10^8	5.164×10^{10}
p_{02}	-1.404×10^9	-1.841×10^8	-2.206×10^9	8.817×10^{10}
p_{30}	-3.985×10^4	-8.251×10^3	-2.668×10^4	-2.286×10^7
p_{21}	-2.358×10^6	8.45×10^4	4.106×10^5	5.996×10^7
p_{12}	7.51×10^7	9.708×10^6	-6.894×10^7	-4.337×10^9

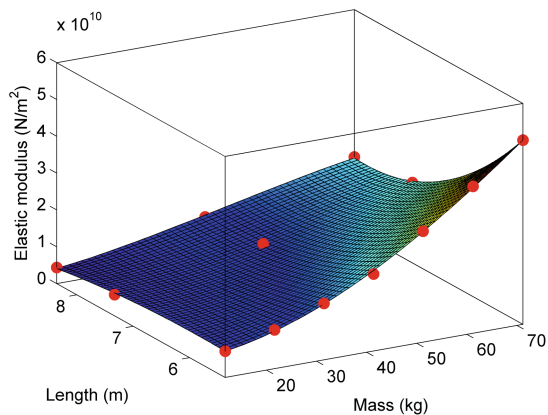


Fig. 7. Surface fitting for E_{L1} with loading condition

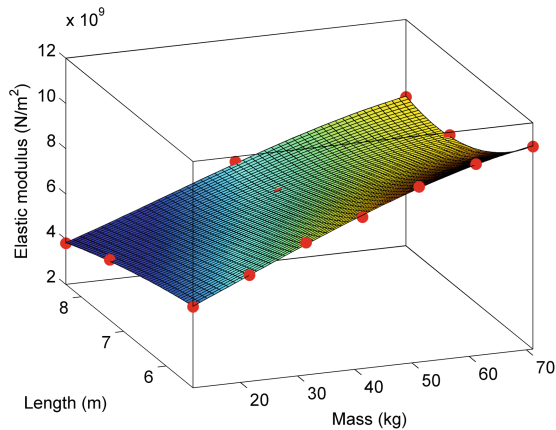


Fig. 8. Surface fitting for E_{UL1} with unloading condition

The change of parameters can be described using polynomial function with two variables, mass and cable length, as in (5).

$$\begin{aligned}
 P(l, m) = & p_{00} + p_{10}m + p_{01}l + p_{20}m^2 + p_{11}ml \\
 & + \dots p_{02}l^2 + p_{30}m^3 + p_{21}m^2l + p_{12}ml^2
 \end{aligned}
 \tag{5}$$

where $P(l, m) = E_{L1}, E_{UL1}, E_{UL3}, \eta_{UL3}$ and all values are listed in Table 3.

In order to examine the trend of dual parameters variation, i.e., mass and cable length, surface fitting is established by using (5). Figure 7 shows the loading elastic modulus E_{L1} which increases with high payload and short cable length. Figures 8, 9 and 10 shows the unloading elastic modulus E_{UL1}, E_{UL3} and viscosity η_{UL3} . In Figs. 8 and 10, E_{UL1} and η_{UL3} have the similar trend with E_{L1} . Although experimentally

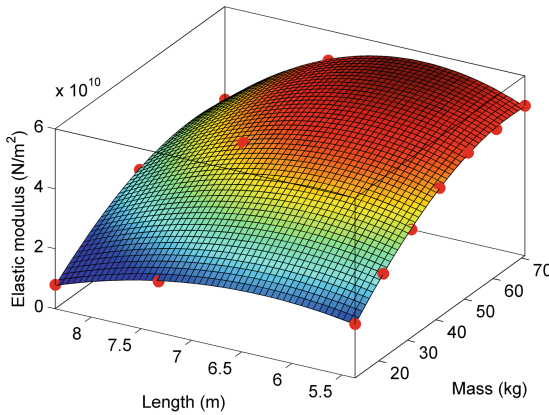


Fig. 9. Surface fitting for E_{UL3} with unloading condition

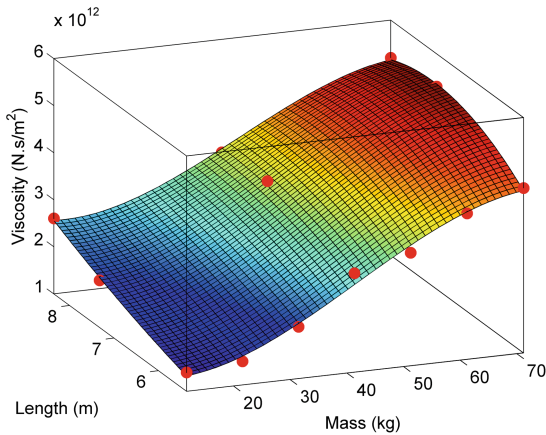


Fig. 10. Surface fitting for η_{UL3} with unloading condition

estimated E_{UL3} increases with high payload and short cable length, its polynomial function does not properly represent the trend of E_{UL3} in Fig. 9. It is expected that more experimental data will improve the function of the surface fitting.

4 Conclusion and Future Works

In this paper, a data based five-element model is proposed for describing creep behavior of polymer cables when loading and unloading. Model parameters are estimated by searching a minimum RMSE of a measured signal and an estimated model comparison. It is found that the parameters are considerably different during loading and unloading period with different payloads and different cable lengths due to the nonlinear properties of polymer cable. Polynomial functions for model parameters are built for fitting the experimental data in a function of mass and cable length. The comparison results between model and experiments in time domain shows reasonable good possibilities of the suggested parametric model utilization. Surface model including both mass and cable length parameters shows that the elastic modulus E_{L1} , E_{UL1} and viscosity η_{UL3} increase with high payload and short cable length. However, the estimation E_{UL3} is needed to be improved by using more experimental data.

In the future, our model will be expanded to cover a wide range of excitations and other factors will be considered as well as the effect of temperature. In addition to the model expansion, the effectiveness of a parameter estimation by minimizing RMSE between our model and experimental data will be quantitatively evaluated by accompanying other simple fitting functions. Also, a model based position control will be implemented for our 8 cable-driven parallel robot system and the expanded cable model will be included as part of dynamic model of our CDPR to compensate errors induced by cable creeping.

Acknowledgments. Research supported by Leading Foreign Research Institute Recruitment Program through the National Research Foundation of Korea (NRF) funded by the Ministry of Science, ICT and Future Planning (MSIP) (No. 2012K1A4A3026740).

References

1. Kawamura, S., Kino, H., Won, C.: High-speed manipulation by using parallel wire-driven robots. *Robotics* **18**(3), 13–21 (2000)
2. Maeda, K., Tadokoro, S., Takamori, T., Hiller, M., Verhoeven, R.: On design of a redundant wire-driven parallel robot WARP manipulator. In: *IEEE International Conference on Robotics and Automation*, pp. 895–900 (1999)
3. Kawamura, S., Choe, W., Tanaka, S., Pandian, S.: Development of an ultrahigh speed robot FALCON using wire drive system. In: *1995 Proceedings of the IEEE International Conference on Robotics and Automation*, vol. 1, pp. 215–220 (1995)
4. Dallej, T., Gouttefarde, M., Andreff, N., Dahmouche, R., Martinet, P.: Vision-based modeling and control of large-dimension cable-driven parallel robots. In: *2012 IEEE/RSJ International Conference on Intelligent Robots and Systems (IROS)*, pp. 1581–1586 (2012)

5. Kraus, W., Schmidt, V., Rajendra, P., Pott, A.: Load identification and compensation for a cable-driven parallel robot. In: Proceedings of International Conference on Robotics and Automation, Karlsruhe, Germany, pp. 2485–2490 (2013)
6. Miermeister, P., Kraus, W., Lan, T., Pott, A.: An Elastic Cable Model for Cable-Driven Parallel Robots Including Hysteresis Effects, pp. 17–28. Springer International Publishing, Switzerland (2015)
7. Miyasaka, M., Haghighipناه, M., Li, Y., Hannaford, B.: Hysteresis model of longitudinally loaded cable for cable driven robots and identification of the parameters. In: Proceedings of IEEE International Conference on Robotics and Automation, Stockholm, Sweden, pp. 4051–4057 (2016)
8. Korayem, M.H., Taherifar, M., Tourajizadeh, H.: Compensating the flexibility uncertainties of a cable suspended robot using SMC approach. *Robotica* **33**(3), 578–598 (2014). Cambridge University Press
9. Seon, J., Park, S., Ko, S.Y., Park, J.-O.: Cable configuration analysis to increase the rotational range of suspended 6-DOF cable driven parallel robots. In: Proceedings of the 16th International Conference on Control, Automation and Systems, Gyeongju, Korea, pp. 1047–1052 (2016)
10. Momoh, J.J., Shuaib-babata, L.Y., Adelegan, G.O.: Modification and performance evaluation of a low cost electro-mechanically operated creep testing machine. *Leonardo J. Sci.* **16**, 83–94 (2010)
11. Czichos, H.: Springer Handbook of Materials Measurement Methods, pp. 303–304. Springer, Berlin (2006)
12. Findley, W.N., Davis, F.A.: Creep and Relaxation of Nonlinear Viscoelastic Materials, pp. 58–62. Courier Corporation (2013)
13. Lurzhenko, M., Mamunya, Y., Boiteux, G., Lebedev, E.: Creep/stress relaxation of novel hybrid organic-inorganic polymer systems synthesized by joint polymerization of organic and inorganic oligomers. *Macromol. Symp.* **341**(1), 51–56 (2014)